International Society for Rock Mechanics and Rock Engineering
Norwegian Group for Rock Mechanics

ISRM International Symposium
Eurock 2025 – Expanding the Underground Space
Trondheim, Norway, 16-20 June
ISBN 978-82-8208-079-8

Non- destructive testing in weathering evaluation- from rock massif to stone sculpture

M. Sokołowska & I. Stan-Kłeczek
Institute of Earth of Science, Faculty of Natural Science, University of Silesia, Sosnowiec, Poland
malgorzata.wrobel@us.edu.pl (email of corresponding author)

Abstract

Stone sculptures exposed to atmospheric factors are subject to weathering processes, which lead to changes in their physical properties over the years. The best way to assess the condition of rock objects is to use non-destructive testing (NDT) methods. One of them is ultrasonic tomography measurement, which is based on measuring the travel time of the ultrasonic wave through the object. The research was done on samples made of Permian granite from a quarry in Strzegom (Poland). The samples come from the same granite block, which was cut on the rectangular blocks. Four samples of size 30 cm x 20 cm x 20 cm were measured in the laboratory, and one was left in open air, where it was exposed to atmospheric factors such as temperature, humidity, rain and snowfall. The tomography measurement was done using PunditLab+ equipment from Proceq company. Transducers with a frequency of 250 kHz were used in the tests. The average ultrasonic wave velocity on the laboratory sample was 4637 m/s, and on the field sample 3223 m/s for the P- wave and 2840 m/s and 2154 m/s for the S- wave. The obtained data were interpreted using the aTom software (1.0.2) to get an image of laboratory and field samples P-wave velocity changes. The measurement of the P- and S- wave velocities made it possible to calculate the dynamic modulus, which provided information on the change in the mechanical strength of the tested objects. The calculated weathering coefficient is 0.3. The Schmidt hammer was also performed, providing additional information and confirming the effect of atmospheric conditions on the sample.

Keywords

Ultrasonic tomography, granite rock, weathering evaluation, Schmidt hammer (max 5 keywords)

1 Introduction

Rocks have different physical properties depending on their formation and their mineral composition. Additionally, their physical properties are affected by cracks and crevices. Recognition of this phenomenon and the effect of cracks on the strength of the mass is necessary due to the use of the obtained results in the construction of tunnels, storage sites or testing the stability of the geological rock mass in engineering studies (Krišťáková and Pandula 1996; Mockovčiaková and Pandula 2003; Hildyard et al. 2005; Colombero et al. 2016; Ghafoori et al. 2018).

Rock material is also used as a finishing material and decorative stone. The attempt to preserve cultural heritage by, for example, analysing the structure's internal structure, possible deterioration zones, and cracks using non-destructive testing methods is of interest. Research is mainly carried out on cultural heritage objects such as columns in churches or building facades (Grazzini et al. 2020; Capizzi and Cosentino 2011; Casula et al. 2021; Zielińska and Rucka 2018; Jo and Lee 2022; Santos-Assunçao 2014; Choi et al. 2016; Pérez-Gracia 2013). It is important to know the influence of atmospheric factors and conditions on the weathering process, to have tools to monitor this process and to know what parameters describing this process and the durability of selected rocks. In order to determine physical parameters and assess the weathering process, elastic wave velocity measurements are performed, among others. Since some methodologies are invasive and destroy or affect the structure, non-destructive testing (NDT) is the best technique. In this article, primarily ultrasonic tomography and the Schmidt hammer were used.

The aim of the study was to compare the physical properties of the weathered sample of granite from Stzregom, Polnad, with those stored indoors using two methods. The samples come from the same granite block and they were cut in the same time.

2 Materials and methodology

The measurements were made on four samples with a length of 30 cm and a section of 20 cm x 20 cm and on one sample from the field with a length 59 - 56 cm, width 21 cm and height 10.5 – 8.5 cm. The samples were cut out from the block of granite rock (Fig. 1 The granite laboratory sample (A) and field sample (B) was cut out from the same block of granite rock (C), performing measurements with P and S-wave transducers (D), signal curve read saved during measurements (E). The field sample comes from the same places as the laboratory samples was outside for 7 years, and it was exposed to changing atmospheric factors. The granite is medium-grained and has a random structure.

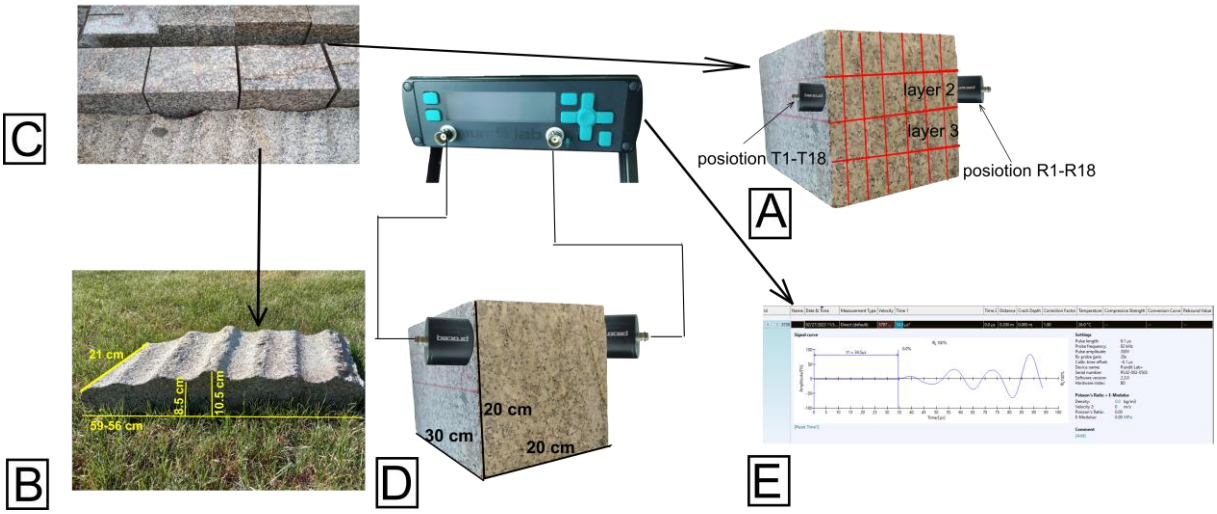

Fig. 1 The granite laboratory sample (A) and field sample (B) was cut out from the same block of granite rock (C), performing measurements with P and S-wave transducers (D), signal curve read saved during measurements (E).

2.1 Ultrasonic measurement

The ultrasonic measurement was carried out using the ultrasonic instrument Pundit Lab+ (Proceq Company). An ultrasonic wave pulse through a rock sample is created at a point on the surface of the test object, and its travel from that point to another is measured. The result of the ultrasound reading is the ultrasonic wave's travel time (t). Way (s) is a travel path length. Therefore, the ultrasound velocity is calculated as v = s/t. The experimental equipment consists of a recorder, transmitter and receiver transducers. The measurements were performed using 250 kHz frequencies. The frequency of the transducers used depends on the sample size and is related to the possibility of performing a measurement on the sample. The size of the object that the wave can measure is ½ - ¼ of the wavelength. This means that for a transducers with a frequency of 250 kHz the smallest distance that can be measured in the sample is 1.6 cm. The applied measurement methodology shows that a distance of 4 cm generates anomalous values. With a 54 kHz probe this distance is 7.4 cm. Which shows that the obtained results would not be error-free visible as places with increased velocity values (Wróbel and Stan-Kłeczek 2023). A fine couplant layer was applied to ensure close contact between the sample's surface and transducers. Using the PunditLink software, the first P-wave and S-wave transit times were manually determined. On the basis of the wave travel path, the P-wave and S-wave velocities were calculated. The S-wave velocity was measured using the same equipment but with S-wave transducers. The measurements were taken for two positions of transducers settings. In the first case, the wave polarization was vertically and in the second case, the wave polarization was horizontally, this corresponded to SH and SV, respectively. The Poisson ratio, Young modulus, bulk modulus, shear modulus were calculated based on average P- and S-wave velocity values. Finally, ultrasonic tomography was performed using the P-wave travel times in the aTom program (1.0.2). The software performs a tomographic analysis based on the geometric shape of the sample and the time of an ultrasonic wave passing through the sample. The software carries out a mathematical interpretation of the results, which are presented as velocity distribution maps (tomograms) of the P-waves along the plane of sections obtained using an iterative calculation procedure type S.I.R.T. (Simultaneous iterative reconstruction technique) (http://ultrasonictomography.com/en/features/).

2.1.1 Laboratory measurements

The first step of measurements is zeroed using a calibration rod that has a designated frequency (24μs). The transmitter transducer was located opposite to the receiver (11x11=121) along the longer edge of the sample, and the same configuration was along the shorter edge (7x7=49). In the first sequence of measurements, the transmitting transducer was in the T1 position, and the receiving head was moved from the R1 to the R11 location (Fig. 1 The granite laboratory sample (A) and field sample (B) was cut out from the same block of granite rock (C), performing measurements with P and S-wave transducers (D), signal curve read saved during measurements (E).. Next, the transmitting transducers were in the T2 position. The receiver transducers were moved from the R1 to the R11 location. The distances between subsequent positions of the centre of the transducer were 2.5 cm. The described data acquisition generates 170 average results for one layer. Because the measurement was repeated 15 times for each transducer's arrangement, we had 2550 data for one layer. Measurements were made for two middle layers. The results were averaged. It improved the signal-to-noise ratio and allowed a more reliable reading of the wave's arrival time.

In the S-wave velocity measurements, the transducers were also located opposite each other. The measurements were performed on the second and third layers at positions T5 - R5, T7 - R7, T14 - R14 and T16 - R16. The distance between subsequent positions of the centre of the transducer was about 5 cm. The described data acquisition generates 8 results for one sample. Because for each transducer's arrangement, the measurement was repeated 30 times (15 times for one direction of polarization and 15 times for the other direction of polarization) so were had 240 data for one sample.

2.1.2 Field sample measurements

The first step of measurements is zeroed using a calibration rod. The transmitter transducer was located opposite the receiver along the longer edge of the sample. The transmitting transducer was in T1 to T18 position. The receiver transducers were moved from the R1 to the R18. The distance between subsequent positions of the centre of the transducer was about 2.5 cm. The described data acquisition generates 18 average results. Just like on the sample in the laboratory each transducer's arrangement, the measurement was repeated 15 times so were had 270 data.

For the S-wave velocity measurements, the transducers were also located opposite each other along the longer edge of the sample. The transducers were in 9 positions. The distance between subsequent positions of the centre of the transducer was about 5 cm. The described data acquisition generates 9 average results for one sample. Because for each transducer's arrangement, the measurement was repeated 30 times (15 times for one direction of polarization and 15 times for the other direction of polarization), so we had 270 data for one sample.

2.2 Schmidt hammer measurement

The measurements were also performed using a Schmidt hammer concreto N-type with an impact energy of 2.207 Nm. The tests were performed in accordance with ISRM suggested method, on a sample in the laboratory and on a sample in the field (Aydin 2008). For the sample in the laboratory, due to the size of the sample, measurements were performed in 4 locations. In each location, 10 rebound were performed, because the rebound values differed from each other by less than 4 units. On the sample from the field, measurements were performed in 18 locations on one side of the sample and in 9 locations on the other side of the sample. For all rebound values, the bounce values were normalized. The method allowed determining the elastic rebound index (R_N).

3 Result and discussion

The measured laboratory samples have similar velocity values for both the second and third layers. Taking into account all laboratory samples, the average velocity for the P-wave was 4637 m/s. In the S-wave velocity measurements, there is no significant difference in velocity for the two different wave polarization directions. There is a clear difference between the velocities measured on the sample and in the field The obtained values are summarized in Table 1.

Table 1 Results from measurements P- and S-wave velocity and Schmidt hammer

Vp [m/s]				**Vs [m/s]**			**Schmidt hammer**
Sample	**Layer**	**mean**	**stand. dev.**	**Polarisation direction**	**mean**	**stand. dev.**	
1	2	4630	270				
	3	4625	230				
2	2	4365	415	mean	2840	65	68
	3	4415	310	parallel	2838	64	
				perpendicular	2842	66	
3	2	4418	300				
	3	4376	290				
4	2	5689	272				
	3	4573	220				
field		3223	320	Mean	2154	244	64 (first side)
				parallel	2115	301	53 (second side
				perpendicular	2192	161	

Changes in the P-wave velocity values in the laboratory and field can be seen in Fig. 2 Ultrasonic tomography of field sample (A) and laboratory sample (B).

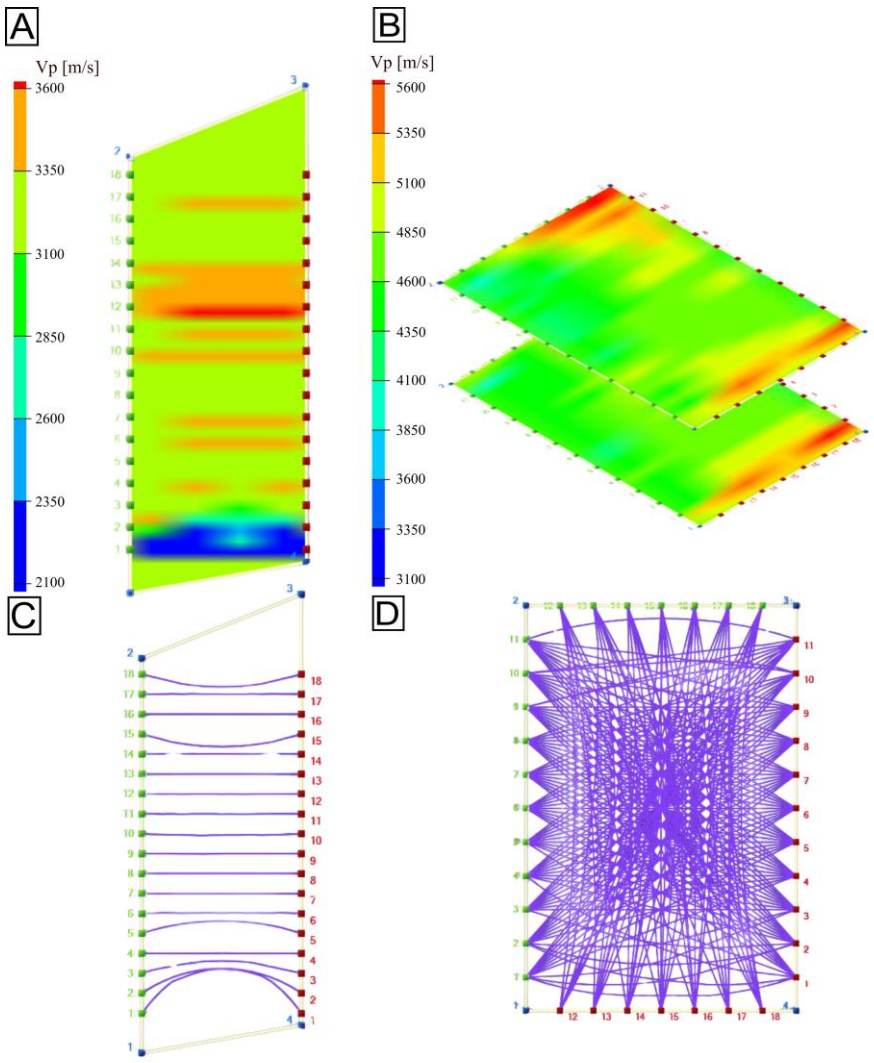

Fig. 2 Ultrasonic tomography of field sample (A) and laboratory sample (B). Rays arrangement for the field sample (C) and laboratory sample (D)

Differences in P-wave velocity are visible in ultrasonic tomography (Fig. 2 Ultrasonic tomography of field sample (A) and laboratory sample (B).The field sample has a small coverage of rays (purple line), which may affect the large number of anomalous velocities (see Fig. 2 Ultrasonic tomography of field sample (A) and laboratory sample (B).The boundary rays are bent what may be a boundary effect. More measurements were taken for the laboratory sample, which allowed for a larger coverage of rays. Anomalous velocities of higher value occur at the edges. In both cases, a deviation of rays was observed in the lower and upper parts (Fig. 2 Ultrasonic tomography of field sample (A) and laboratory sample (B). Rays arrangement for the field sample (C) and laboratory sample (D)This may be the result of difficulties in fitting the theoretical model to the data by the program or the occurrence of a boundary phenomenon.

The Student's t test was used in order to verification of differences between P- wave seismic velocities. This test allows to check the hypothesis whether the average values of P-wave velocity of the two periods are equal. It was assumed that the distribution of the mean value of velocity in both periods is a normal distribution of different variances. The test was performed using a data analysis tool. The test was done for field sample and laboratory sample. The null hypothesis was established that the mean value of P - wave velocities were equal, and the alternative hypothesis was established that they were different. The level of significance was = 0.5. The number of degrees of freedom was 29 and the P-value was $2.5*10^{-10}$. The results show that there is evidence to reject the null hypothesis, that is the mean values of P-wave velocity values obtained for two times intervals are difference.

There are small differences in the hammer rebound values for the field and laboratory samples (Table 1 Results from measurements P- and S-wave velocity and Schmidt hammer. The lower value and greater scatter of rebound values are on one side of the sample. This is a rough surface, so this may be

due to loss of impact energy. The second possibility is the stronger effect of atmospheric conditions, which caused a faster weathering process (Aydlin and Basu, 2005).

Table 2 Result for modulus calculation shows the calculated moduli for the 4 laboratory samples and the field sample. Since the velocity values did not differ between the samples, the P- wave velocity was averaged for the entire sample. The density value for granite was calculated based on the sample mass and volume. Since the samples came from the same location, a single density value of 2.703 g/cm3 was assumed for all measurements.

Table 2 Result for modulus calculation

	Sample 1	**Sample 2**	**Sample 3**	**Sample 4**	**Field Sample**
Possion ratio (ν)	0.20	0.14	0.14	0.19	0.10
Young's modulus (E)	52 GPa	50 GPa	50 GPa	52 GPa	28 GPa
Bulk modulus (K)	29 GPa	23 GPa	23 GPa	28 GPa	11 GPa
Shear modulus (μ)	22 GPa	22 GPa	22 GPa	22 GPa	13 GPa

The Yong modulus values for samples 1 - 4 are 50 - 52 GPa, for field sample has a much lower value 28 GPa. A similar situation was observed for the Bulk modulus (sample 1 - 4: 23 – 29 GPa, field sample 11 GPa) and Shear modulus (sample 1 - 4: 22 GPa, field sample 13 GPa).

Based on the work of Jo and Lee (2022), the weathering coefficient was calculated. The coefficient is based on the ultrasonic velocity value. The change in the K coefficient value over time is influenced by, for example, the type of rock, density, porosity and microcrack expansion. The value of the coefficient increases with the increase in the degree of rock weathering. In the conducted studies, the K coefficient value was 0.30.

4 Conclusion

Ultrasonic tomography and Schmidt hammer rebound methods allowed for the assessment of rock weathering. Ultrasonic wave velocity measurements of P- and S-wave are lower for field sample that for the laboratory samples. Calculated Young's module, shear modulus, and bulk deformation modulus are the same for laboratory samples, but there is a significant drop in the value for the field sample what can be the result of weathering. The obtained results of the Student's t test proved that the differences in velocity values in the samples are statistically significant and therefore it can be concluded that the field sample was affected by the weathering process. The results demonstrate that the physical properties of the tested samples vary under the influence of atmospheric factors.

Funding: This research was funded by the National Science Centre, Poland (NCN), grant number 2024/53/N/ST10/02459.

Acknowledgments: We thank the Institute of Geonics of the Czech Academy of Sciences (Ostrava, Czech Republic) for lending S-wave transducers.

References

Aydin A (2008) ISRM Suggested Method for Determination of the Schmidt Hammer Rebound Hardness: Revised Version. In: Ulusay, R. (eds) The ISRM Suggested Methods for Rock Characterization, Testing and Monitoring: 2007-2014. Springer, Cham. DOI: 10.1007/978-3-319-07713-0_2

Capizzi P, Cosentino P L (2011) Electromagnetic and ultrasonic investigations on a Roman marble slab. Journal of Geophysics and Engineering, 8(3): pages: 117-125. DOI: 10.1088/1742-2132/8/3/S11Casula G, Fais S, Cuccuru F, Bianchi M G, Ligas P, Sitzia A (2021) Decay detection in an ancient column with combined close-range photogrammetry (Crp) and ultrasonic tomography. Minerals, 11(10), 1114. DOI: 10.3390/min11101114

Choi H, Ham Y, Popovics J S (2016) Integrated visualization for reinforced concrete using ultrasonic tomography and image-based 3-D reconstruction. Construction and building materials, 123: pages: 384-393. DOI: 10.1016/j.conbuildmat.2016.07.010

Colombero C, Comina C, Umili G, Vinciguerra S (2016) Multiscale geophysical characterization of an unstable rock mass, Tectonophysics 675: pages 275-289. DOI: 10.1016/j.tecto.2016.02.045

Ghafoori M, Rastegarnia A, Lashkaripour G R (2018).Estimation of static parameters based on dynamical and physical properties in limestone rocks, Journal of African Earth Sciences 137: pages 22-31. DOI: 10.1016/j.jafrearsci.2017.09.008

Grazzini A, Fasana S, Zerbinatti M, Lacidogna G (2020) Non-destructive tests for damage evaluation of stone columns: The case study of Sacro Monte in Ghiffa (Italy). Applied Sciences, 10(8), 2673. DOI: 10.3390/app10082673

Hildyard M W, Young R P, Collins D C, Pettitt W (2005) Seismic wave propagation to diagnose the state of fracturing, The Journal of The South African Institute of Mining and Metallurgy 105: pages: 437-446Jo Y H, Lee C H (2022) Ultrasonic properties of a stone architectural heritage and weathering evaluations based on provenance site. Applied Sciences, 12(3), 1498. DOI: 10.3390/app12031498Krišťáková Z, Pandula B (1996) The relation between laboratory and in situ determined dynamic moduli of rock, Acta Montana 9 (100): pages:201-205

Mockovčiaková A, Pandula B (2003) Study of the relation between the static and dynamic moduli of rocks, METABK 42(1): pages 37-39. DOI: 10.1088/1742-2132/8/3/S11

Pérez-Gracia V, Caselles J O, Clapés J, Martinez G, Osorio R (2013) Non-destructive analysis in cultural heritage buildings: Evaluating the Mallorca cathedral supporting structures. NDT & E International, 59: pages: 40-47. DOI: 10.1016/j.ndteint.2013.04.014

Santos-Assunçao S, Perez-Gracia V, Caselles O, Clapes J, Salinas V (2014) Assessment of complex masonry structures with GPR compared to other non-destructive testing studies. Remote Sensing, 6(9): psges 8220-8237. DOI: 10.17509/ajse.v2i2.37975

Wróbel M, Stan-Kłeczek I (2023) Measurement of the velocity of ultrasonic waves of different frequencies on granite sample (Strzegom, Poland). Exploration Geophysics, Remote Sensing and Environment, Issue 2023/1

Zielińska M, Rucka M (2018) Non-destructive assessment of masonry pillars using ultrasonic tomography. Materials, 11(12), 2543. DOI: 10.3390/ma11122543

An online reference title. http://ultrasonictomography.com/en/features/. Accessed Date: 14.12.2024)